

Analysis of *Arabidopsis* defensin-like genes and ovule development during fertilization and *Fusarium* infection

K. Spalvins* and D. Blumberga

Riga Technical University, Institute of Energy Systems and Environment,
Azenes street 12/1, LV 1048, Riga, Latvia

*Correspondence: kriss.spalvins@rtu.lv

Abstract. Defensins are small, highly stable antimicrobial peptides. Many defensin-like (DEFL) peptides found in flowering plant *Arabidopsis thaliana* are believed to have role in either natural immunity or cell-to-cell communication during fertilization. However, little is known about the DEFL peptides and their functions during these events. The goal of this work is to investigate the genes encoding selected DEFLs by observing their expression patterns during fertilization and *Fusarium graminearum* infection. According to the results 4 selected genes of interest (GOI) are downregulated after fertilization and infection and mock treatments are causing degradation and delay of development in treated ovules.

Key words: defensins, defensin-like peptides, development, double fertilization, *Fusarium graminearum* infection.

INTRODUCTION

Defensin-like genes form a large multigene family of more than 300 DEFL genes in the flowering plant *Arabidopsis thaliana*. These DEFL genes encode cysteine-rich peptides (CRPs) that are highly diverse and have conserved pattern of cysteine residues (Takeuchi & Higashiyama, 2012). Even though DEFLs are diverse, they mostly function in disruption of microbial membranes and have a ligand-like activity for cellular communication (Stotz et al., 2009). It is believed that DEFL genes have roles in male/female interactions such as intercellular communication during double fertilization and host/parasite interplays like defense reactions against pathogens (Ganz, 2003; Takeuchi & Higashiyama, 2012).

It is reported that *Arabidopsis* is applicable for studying *Fusarium* head blight (FHB), a devastating disease of cereal crops caused by *Fusarium* fungus. It is estimated that this pathogen causes huge economic losses each year worldwide (McMullen et al., 1997; De Wolf et al., 2003). Infection affects the amino acid composition, thus resulting in shriveled kernels (Beyer & Aumann, 2008). Grains harvested from infected plants are contaminated with dangerous mycotoxins, such as protein biosynthesis inhibiting deoxynivalenol and an estrogenic mycotoxin zearalenone (Häggbloom & Nordkvist, 2015). In livestock, these toxins cause vomiting, reproductive defects, and liver damage and are considered harmful to humans as well (Gautam & Dill-Macky, 2011).

Mainly due to large size of genomes in cereal species and expensive resources required to research gene function in these plants, molecular basis of resistance to FHB is poorly understood. *Arabidopsis* has been noted for its potential for translational research in cereals (Brewer & Hammond-Kosack, 2015). Research done in *Arabidopsis* greatly reduces the time investment and expenses of the research due to short life cycle and small genome size of the model organism (Urban et al., 2002). The goal of this work is to investigate the *Arabidopsis thaliana* genes, encoding selected DEFLs, by observing dynamic change in expression of corresponding gene putative promoters during fertilization and *Fusarium graminearum* infection.

MATERIALS AND METHODS

In order to investigate expression and role of defensin-like proteins from *Arabidopsis* during fertilization and in the immune response to *Fusarium* various experiments were conducted. The whole research was divided into three parts (series of experiments). First part included the creation and analysis of marker lines to follow the activity of the corresponding putative promoters *in planta*. The second series of experiments were divided further into two sub-studies (pollination studies and pollination followed by infection (pollination-infection) studies). In this series marker lines were used to measure green fluorescence protein (GFP) signal intensity and quantify it in dissected ovules under the microscope. The third series were developmental studies where by using homogeneous marker lines the dynamic effect of various treatments on ovule development was observed. All experiments in detail are described in author's Master thesis available at University of Latvia Union Catalogue (Spalvins, 2016).

Marker lines (first series of experiments)

Paralogous genes identified by Takeuchi & Higashiyama (2012) were picked as a starting point. These 71 genes were then compared with the data of Huang et al. (2015) where expression profiles of 572 CRPs in ovule samples were analyzed. 53 of initial paralogous genes were also analyzed in these ovule samples, of which 18 genes followed the expression pattern of reaching peak expression at 6 hours after pollination. These genes were further investigated in publicly available expression database (Genevestigator) (Zimmermann et al., 2004). By analyzing mRNA sequencing data genes AT2G40995; AT5G38330; AT5G43285; AT1G60985 were picked because of the expression localization in developed flower and increased expression during treatment with various pathogens.

Putative promoters of genes AT2G40995; AT5G38330; AT5G43285; AT1G60985 were used for the creation of the marker lines.

Construct used for creation of the marker lines was pAT*G*****:NLS>(*x)eGFP line * (p – putative promoter, AT – *Arabidopsis thaliana*, AT* – chromosome number, G***** – gene number, NLS – nuclear localization signal (signal only expressed in nucleus), eGFP – enhanced green fluorescent protein, (*x) – number of tandem repeats of eGFP, line * – line number), p***** – * (p – putative promoter, ***** – gene number, * – line number) in short.

Consecutive scheme of making and analyzing marker lines is shown in Fig. 1.

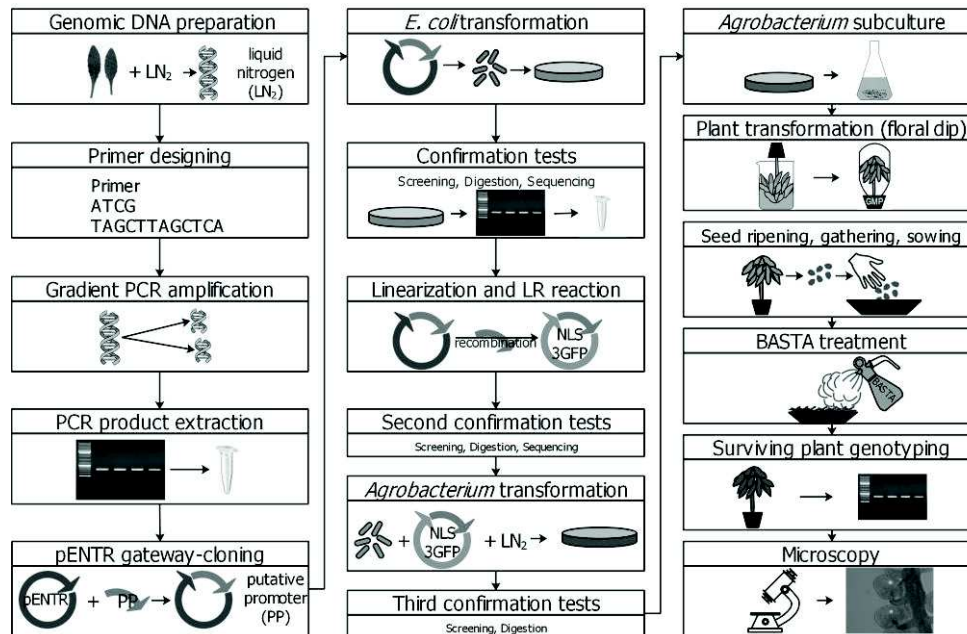


Figure 1. Overall scheme of creating and analyzing marker lines.

GFP signal quantification (second series of experiments)

In this series previously selected marker lines from the first series were used in order to investigate dynamic change of GFP signal intensity under such events as fertilization and infection. In order to have biological replicates for each gene two different lines were used.

In pollination studies flowers of the marker line plants were emasculated and pollinated. Pollinated pistils were collected and ovules dissected to measure changes in GFP signal intensity under the fluorescence microscope at 0 hours after pollination (HAP), 8 HAP, 24 HAP, 48 HAP. In Fig. 2, scheme of GFP signal quantification for pollination studies is shown.

In pollination-infection studies at specific time periods after emasculatation and pollination, plants were infected with transgenic plant pathogen *Fusarium graminearum* DsRed(Fg8/1) and kept for 1, 2 or 3 days after infection (DAI) under moist conditions suitable for fungal growth.

Two controls were used in these studies – control and mock treatment. Control samples were only emasculated and pollinated with no other treatment applied. Mock treatment received exactly the same treatment as infection samples, only difference being that no pathogen was added in the mixture where plants were dipped in. After letting infection spread for 1, 2 and 3 days plants were removed from treatment chambers. In Fig. 3 scheme of GFP signal quantification for pollination-infection studies is shown.

Quantification process is described in detail in the next two sections: microscopy; signal quantification using ImageJ (Fiji) (Rasband, 2009).

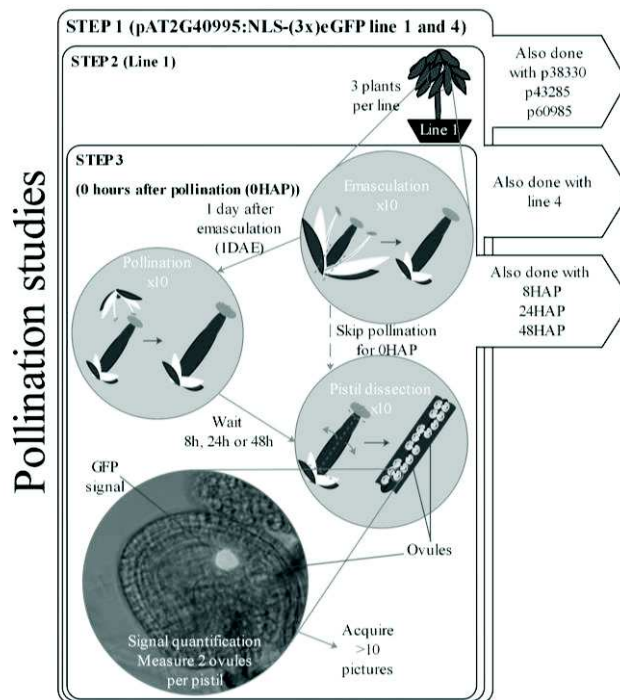


Figure 2. Overall scheme of GFP signal quantification for pollination studies.

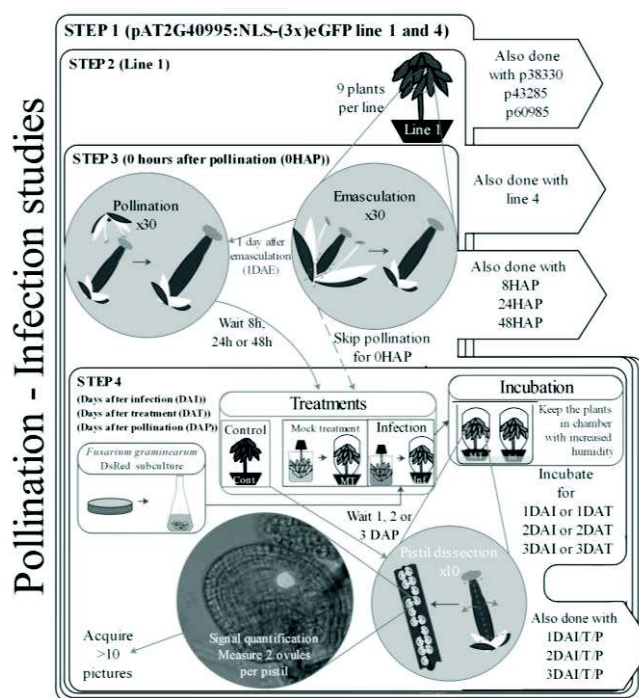


Figure 3. Overall scheme of GFP signal quantification for pollination-infection studies.

***Fusarium graminearum* DsRed (Fg8/1) Infection**

Initially *Fusarium* was cultured in 5 g L⁻¹ and 7.5 g L⁻¹ of wheat media. Cultures were incubated in darkness at 22 °C for 1 week with moderate shaking. Before liquid *Fusarium* culture was set, additional infected potato dextrose agar (PDA) plates were prepared by spreading fungi with an inoculation loop on freshly made plates.

The concentration of *Fusarium* spores within the media was estimated with the following procedure: 50 mL of a liquid culture were filtered through autoclaved cotton gauze and centrifuged for 15 min at 22°C at 5,000 rpm. The supernatant was carefully removed, 30 mL of water were added to resuspend the pellet. The concentration of *Fusarium* spores was calculated by applying 20 µl of solution on the upper part of a counting chamber and then closing it with a coverslip. Spores within the gridded glass chamber were counted under the Nikon TS100 microscope. By knowing the volume in which the cells were initially re-suspended, the number of squares where spores were counted and the number spores within each square it was possible to calculate concentration. After that 1% Tween infection mixture was prepared in a beaker by diluting with water the *Fusarium* solution to a concentration of $\sim 9 \times 10^5$ spores mL⁻¹ in total volume of 300 mL.

Infection itself was done by floral dipping. After dipping, plants were covered with plastic bags and put into a treatment chamber (sealable 500 x 400 x 298 mm plastic box). Before closing the chamber, the bottom was thoroughly sprayed with water in order to keep humidity high. Other long day growth conditions remained as previously described. The treated plants were kept in the chamber for 1 DAI, 2 DAI, 3 DAI before collecting the treated pistils. The mock treatment proceeded as previously described, but without *Fusarium* on the dipping medium.

Uninfected control plants were emasculated and pollinated as previously described. While infected and mock treatment plants were kept in the treatment (incubation) chamber, control plants were kept in normal growth conditions for the same period of time before gathering the pistils.

Microscopy

Dissection under the stereo microscope was performed by fixing the pistil on double-sided adhesive tape and cutting with a syringe needle. Dissected ovules were put on new slide on 30 µl droplet of 10X PBS buffer and covered with a cover glass.

A method of quantification was developed to acquire data from dissected ovules. The exact exposure time was chosen based on properties of the marker lines. For example, if expression was not very intense the signal was weak, thus higher exposure time was necessary to document it. Because the aim of these experiments was to capture dynamic signal changes over time, the specific signal change after fertilization had to be taken in to consideration. If signal intensity decreased after successful fertilization, then it was crucial to choose such exposure time which would still be sufficient to capture presence of the signal even after expression decreased. It was also important to avoid picking high exposure time because that would result in oversaturation of the signal, thus calculated values of these oversaturated pictures could not be considered accurate.

Taking all these factors into consideration exposure times for each marker lines were chosen (Table 1).

Table 1. Specific exposure times for signal quantification of the candidate maker lines

Marker line	Exposure time (Chanel 2*)
p38330 line 1 and 4	200 ms
p40995 line 1 and 4	300 ms
p43285 line 2 and 17	1,000 ms
p60985 line 1 and 18	200 ms

*for additional information see Table 2.

Supporting information

Table 2. Settings used for Axio imager M2 microscope

Settings	
	10x/0.45 M27
	20x/0.8 M27
	40x/1.4 Oil DIC (UV) VIS-IR M27
Camera	Axiocam 503
Camera adapter	1x Camera adapter
Channel 1. (Default channel used in sample analysis and imaging)	
Reflector	Analy. DIC Trans.light
Contrast method	Brightfield
Light source intensity	2–6 Volt
Channel name	TL Brightfield
Channel color	White
Exposure time (depending on the sample)	5 ms – 1 s
Binning mode	1.1
Channel 2. (If sample had GFP marker in it, then used in combination with channel 1)	
Reflector	38 HE Green Fluorescent Protein
Beam splitter	495
Filter ex. wavelength	450–490
Filter em. wavelength	500–550
Contrast method	Fluorescence
Channel name	EGFP
Channel color	Green
Excitation wavelength	488
Emission wavelength	509
Exposure time (depending on the sample)	20 ms – 1 s
Binning mode	1.1
Channel 3. (If GFP sample was infected with <i>Fusarium graminearum</i> DsRed, then used in combination with channel 1 and 2)	
Reflector	43 HE DsRed
Beam splitter	570
Filter ex. wavelength	538–562
Filter em. wavelength	570–640
Contrast method	Fluorescence
Channel name	DsRed
Channel color	Red
Excitation wavelength	545
Emission wavelength	572
Exposure time (depending on the sample)	100 ms – 1 s
Binning mode	1.1

Stacked pictures of the single ovule showing signal were taken at 40x magnification using an Axio Imager M2 microscope (see Table 2. for microscope settings). When the stacked pictures of the treated marker lines were taken, quantification could be done in ImageJ. Stacked pictures were extended to more dimensions to create hyperstack multidimensional images. Whole sets of images were projected in such a way that only the highest value pixels were shown, thus creating a single picture which projected only the maximum values of the stack. After creating these maximum projection images the values of the signal were measured and the overall value of each of the signals was calculated by subtracting its value from the mean value of the background.

Signal quantification using ImageJ

Following steps were performed in order to quantify the GFP signal from the marker lines: a stacked image of 30 pictures was acquired (Fig. 4).

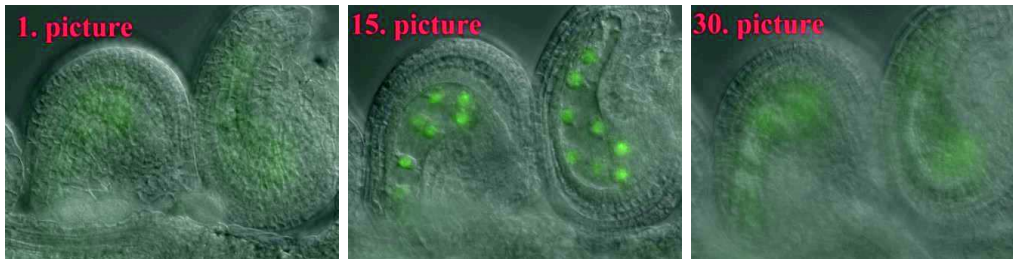


Figure 4. Example of pictures 1., 15. and 30 within single stacked image.

In ImageJ, the stacked image was opened and converted from image to hyperstack by going to Image/Hyperstacks/Stack to Hyperstack. In Convert to HyperStack window following settings were inputted: Order: xyczt(default); Channels (c): 2; Slices (z): 30; Frames (t): 1; Display Mode: Color. After that image projecting the pixels of highest intensity was acquired by going to Image/Stacks/Z Project and in ZProjection window following settings were inputted: Start slice: 1; Stop slice: 30; Projection type: Max Intensity (see Fig. 5).

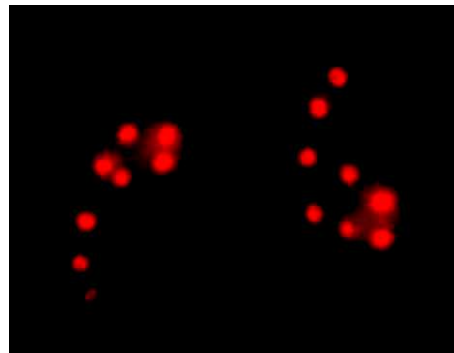


Figure 5. Example of stacked image projecting the pixels with highest intensity of all 30 pictures that the stacked image consisted of.

In the created image every nucleus that was showing GFP signal was circled around by using elliptical or polygon selection tool. After circling single nucleus M key was tapped in order to measure the intensity and T key was tapped in order to save the selection in ROI manager. For every nucleus measured, 5 same size circles around each nucleus were measured in order to acquire the background value (Fig. 6.).

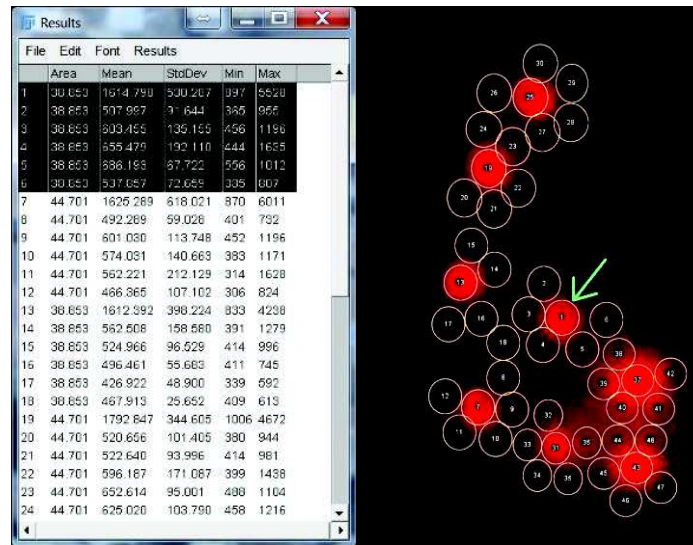


Figure 6. Example of nucleus signal and background circling (left) and intensity measurement acquisition in ROI manager (right).

The average value of the five background measurements was subtracted (see example in Fig. 6 (right)). Results, Mean column: rows 2–6 (average of 5 measurements – 598.196)) from the value of the nucleus (Results, Mean column: row 1 (1614.798)). Thus the signal intensity of single nucleus was acquired (See example in Fig. 6 (right)). Calculated signal intensity of Nucleus 1 (green arrow) is 1016.602). Actions were repeated with every nucleus.

Mean value of all nuclei in single ovule represent single n (see Fig. 9).

Developmental studies (third series of experiments)

The third series of experiments were developmental studies where by using homogeneous marker lines the dynamic effect of pollination-infection treatments on ovule development was observed. In the beginning of these experiments, homogenous plants of the marker lines needed to be found. By using the data from pollination studies (second series of experiments) it was decided that pAT1G60985:NLS-(3x)eGFP line 1 was perfectly suited for the use as homogenous marker line with strong expression long after fertilization (see Fig. 9).

The plants were treated as described before in thesecond series of experiments for pollination-infection studies. The aim was to gather 10 pistils from each condition, dissect them and count, under the microscope, in what stages the ovules were. Fig. 7 represents how ovules looked like to be counted as being at one of the developmental stages. The following stages were recorded for each corresponding condition observed when looking at dissected ovules: degraded; 0 HAP/8 HAP; 10 HAP/12 HAP; 24 HAP; 48 HAP; 72 HAP; 96 HAP. Since pictures for this studies were taken at 10x magnification the ovules that looked like 0 or 8 HAP in this studies were counted in single data set because it was impossible to tell them apart at such a small magnification. Looking at the ovules and count them on larger magnification was not possible since capturing pictures of 10 pistils at every condition at 10x magnification already created

data set of ca. 1,000 pictures. The ovules that looked like 10 and 12 HAP were also counted together because these ovules represented very small set of overall data (only 0.4–8.9% of all ovules counted; see Fig. 12).

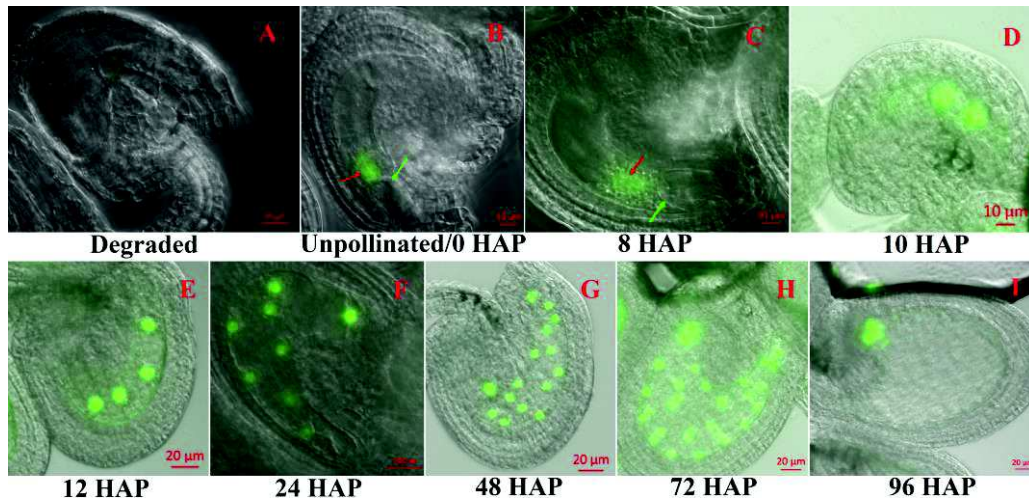


Figure 7. Developmental stages of the *Arabidopsis thaliana* ovules. HAP – hours after pollination. Green spots – GFP signal in central cell nucleus. A – degraded ovule, signs of degradation: ovule decrease in size (A compared to B); disintegration of outer and inner integuments; central cell is left covered with only a thin cell layer of endothelium. B – unpollinated/0 HAP, signs of unpollinated ovule: central cell nucleus (red arrow) still next to egg cell (green arrow). C – 8 HAP, signs of early pollination: central cell nucleus (red arrow) starts to move away from egg cell and synergids (green arrow). D – 10 HAP, first division of central cell nucleus (2 nuclei visible). For every following stage (E, F, G, H) number of GFP signals (number of visible central cell nuclei) doubles. I – 96 HAP, separate nuclei are not discernible anymore (picture taken 5 days after pollination was performed).

RESULTS AND DISCUSSION

Microscopy of the GFP marker lines

Individual T1 transgenic plants that survived BASTA treatment were marked and considered as individual line of the specific gene promoter construct. At the onset of flowering, pistils were dissected to check for the presence of the GFP signal in the ovules. For each of the four DEFL gene (AT2G40995; AT5G38330; AT5G43285; AT1G60985) marker lines, two lines that showed the strongest signal were picked to grow the T2 generation for further studies (see Table 3). Most of the T2 generation marker lines showed GFP signal in the ovules, with majority of those lines showing signal in the nucleus of the central cell before (Fig. 8, A) and after (Fig. 8, B) fertilization suggesting that these genes might have some role in fertilization or development. Marker lines pAT5G43285:NLS-(3x)eGFP line 2 (p43285-2) and line 7 (p43285-7) showed signal in synergids (Fig. 8, C).

Signal smearing in the T2 generation of pAT2G40995:NLS-(3x)eGFP line 4 (p40995-4) can be seen in Fig. 8, E, where smeared signal (red arrow) is visible in the central cell, but it is not inside the nucleus (blue arrow) of the expressing cell even though

GFP had a signal for nuclear localization (NLS). T1 generation was showing proper signal, but analysis of the next generation suggested that marker line is not stable and thus unusable any further.

Table 3. Marker lines that were picked for further studies

Putative promoter DEFL gene marker lines	In short
pAT2G40995:NLS-(3x)eGFP line 1 and 4	p40995-1, p40995-4*
pAT5G38330:NLS-(3x)eGFP line 1 and 4	p38330-1, p38330-4
pAT5G43285:NLS-(3x)eGFP line 2 and 7	p43285-2, p43285-7
pAT1G60985:NLS-(3x)eGFP line 1 and 18	p60985-1, p60985-8

* Unstable in T2 generation.

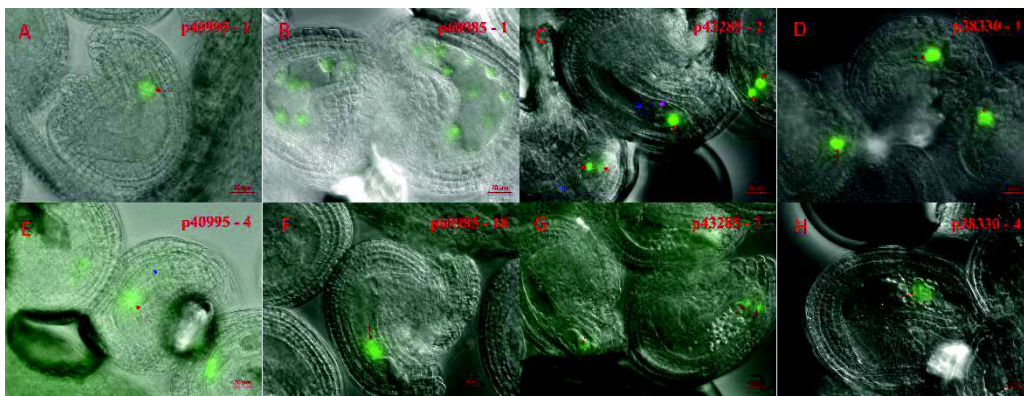


Figure 8. Example of signal expression in ovules of pATxGxxxxx:NLS-(3x)eGFP marker lines. A: red arrow – GFP signal in central cell nucleus; B: green regions – signal in central cell (endosperm) nuclei after fertilization; C: red arrow – GFP signal in synergids, blue arrow – central cell nucleus, violet – egg cell nucleus; D, F, G, H: red arrow GFP signal in central cell nucleus; E: red arrow – smeared GFP signal, blue arrow – central cell nucleus.

GFP signal quantification studies

In general, data acquired from pollination studies suggest that for all four genes promoter activity is being downregulated after fertilization (Fig. 9). In the two pAT5G38330 transgenic lines a noticeable upregulation was observed at 8 HAP (Fig. 9, B), suggesting that this is characteristic of this specific gene during fertilization. Upregulation at 8 hours after pollination (HAP) suggests that AT5G38330 is involved in fertilization related process in the female gametes.

A trend of downregulation for the promoters of genes, pAT2G40995 and pAT5G43285 is observed in all of the respective lines (Fig. 9, A and C). Unfortunately, because there is only one line analyzed for AT2G40995, we cannot say for sure if this is a common property of this particular gene promoter. In relation to gene promoter pAT5G43285, both lines show the same trend of downregulation (Fig. 9, C). This data suggests that the genes are downregulated before fertilization occurs. For *Arabidopsis thaliana* it is known that fertilization takes place 6–8 HAP (Gooh et al., 2015). Therefore our data suggests that, unlike pAT5G38330 gene promoter, which has its peak expression during fertilization, pAT5G43285 has a role in the prefertilization events.

Because there is no data for earlier and intermediate time points like 2 HAP, 4 HAP, 6 HAP and 10 HAP. However, our observations correspond very well with other reports (Huang et al., 2015), thus proving that both our assumptions and quantification method are accurate.

GFP signal intensity change over time HAP

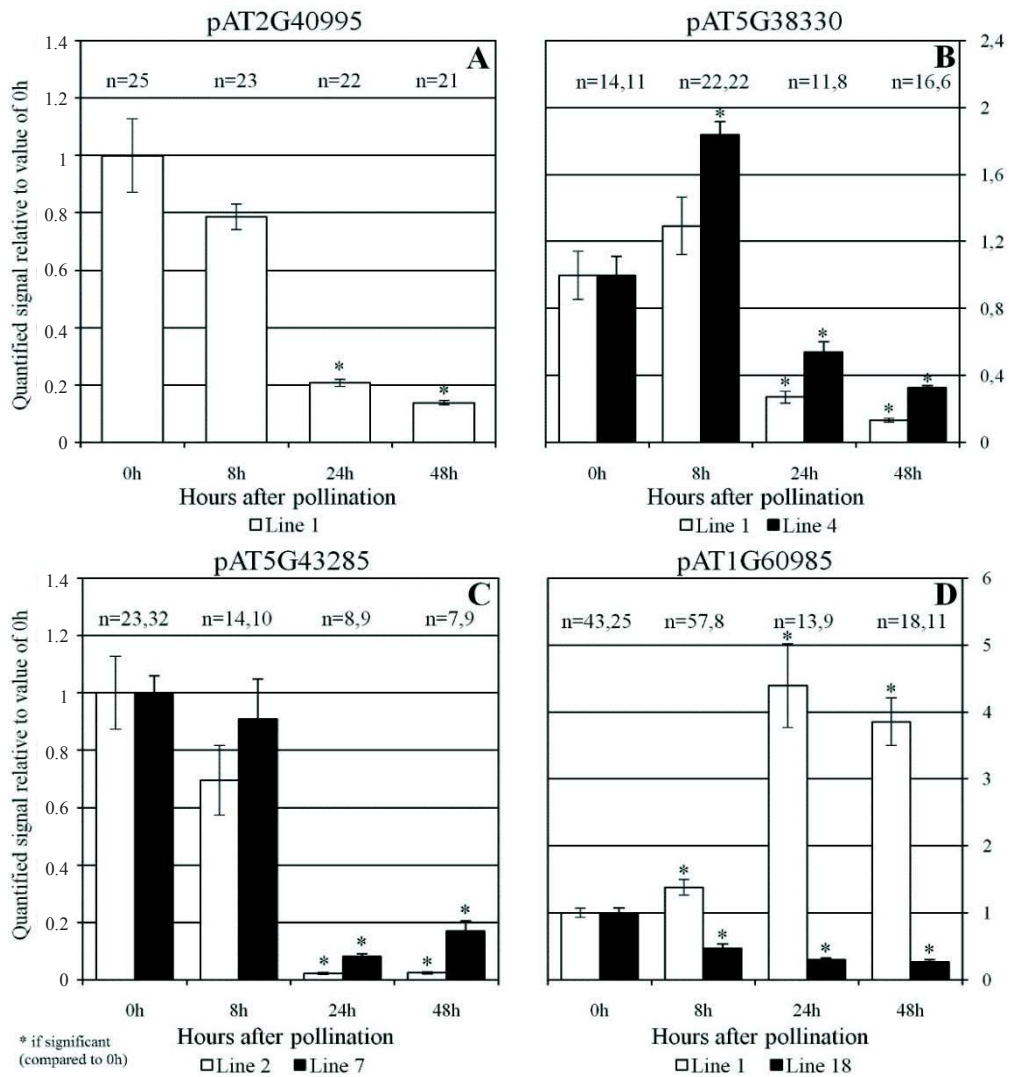


Figure 9. Pollination studies – GFP signal quantification of candidate marker lines at different time points after pollination. Columns represent the mean of the measured signal in multiple ovules (n – number of ovules), error bars represent the standard deviation of the data set. Significance test – One-Way ANOVA; unequal variance t-Test ($p < 0.05$). Note: 24 h and 48 h ovule samples had multiple nuclei with GFP signal in them, thus each n here represent mean of all nuclei signals within single ovule (for more detail see Fig. 7); also note the different scalings of y axes.

Gene promoter pAT1G60985 proved to be very problematic in these studies, because each of the lines show completely opposite trend of promoter activity (Fig. 9, D). With this data alone it is not possible to conclude which trend is representative of the actual properties of expression. If we compare our promoter activity data with the expression patterns of AT1G60985 during and after fertilization reported by Huang et al. (2015), it becomes clear that marker line p60985 – 18 accurately represent the nature of the gene. Concerning line 1 of pAT1G60985, we cannot use it to investigate the specific activity of the promoter for gene AT1G60985. Unlike line 18, it is active after fertilization takes place, showing increase in signal intensity as high as 4 fold at 24 HAP and 48 HAP when compared to the control value of 0 HAP (unpollinated) (Fig. 9, D). This peculiarity was perfect for using this line in developmental studies, where it was crucial to have strong signal after fertilization in order to make it easier to recognize the stage ovules are in (see Fig. 7).

In general, this study relies on the expression of gene promoter not the gene itself and thus might not be very representative of the characteristics of the actual genes in question, but because this method is relatively easy to perform, GFP signal intensity quantification is a good starting point for investigating the conditions in which the genes of interest might be transcribed.

In general, we propose ovule degradation takes place when ovules do not get fertilized for certain period of time. In our case first signs of degradation were usually documented 3 days after emasculum. If we take a look at ovules that have been emasculated and unpollinated in mock and infection treatments for 2 days, which means that since emasculations 3 days have passed, we can see morphological changes in ovules such as: ovule decrease in size (Fig. 10, A compared to C); disintegration of outer and inner integuments (Fig. 10, D, E, F); central cell is left covered with only a thin cell layer of endothelium (Fig. 10, E, F). Because all ovules in Fig. 10 were not pollinated, but degradation was present in both infected (Fig. 10, D, F) and mock treated samples (Fig. 10, C, E), it suggested that the cause for degradation might be the outcome of ovules not being fertilized.

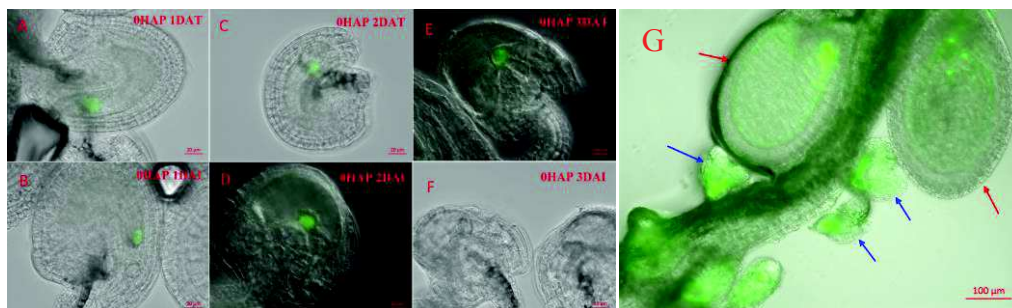


Figure 10. pAT2G40995:NLS-(3x)eGFP in pollination-infection studies. Ovule ageing and degradation. Signs of degradation: ovule decrease in size (A compared to C); disintegration of outer and inner integuments (D, E, F); central cell is left covered with only a thin cell layer of endothelium (E, F). HAP – hours after pollination; DAI – days after infection; DAT – days after mock treatment. Degradation of unfertilized ovules while fertilized ones continue developing (G). Red arrow – fertilized ovules (~120 hours after pollination); blue arrow – unfertilized, degraded ovules.

Unlike those ovules that were fertilized and resulted in normal seed development, unfertilized ovules probably degrade because they are not supplied with nutrients. To support this idea we can see in the Fig. 10, G how in the same ovary unfertilized ovules degrade while the fertilized ones continue development.

When observing the overall situation in the dissected ovules, degradation seemed more severe in samples that were infected when compared to the mock treatment samples (Fig. 10, C compared to D, E compared to F). This suggested the need for a detailed morphological characterization of ovule morphology before and after pollination and during infection.

Overall degradation would not have been a problem in these studies if it would not have affected the quality of the GFP signal. However in the 2, 3 DAI and DAT samples it was very difficult to find any ovules with signal in them. Most of the ovules in these samples looked like the ones seen in Fig. 10, E and F, substantially degraded and with no GFP signal.

Because initial 0 HAP pictures suggested that ovule degradation is caused by prolonged lack of pollination we also documented pistil samples 8 HAP, 24 HAP, 48 HAP which later on were subject to either 1, 2 and 3 days infection with *Fusarium* (1, 2, 3 DAI) or 1, 2, 3 days mock treatment (1, 2, 3 DAT). These samples got fertilized 1 day after emasculation and thus should not be affected by ovule degradation. By looking at these samples we found that, indeed, degradation was observed less frequently, but ovules were in very different developmental stages within a single pistil (Fig. 11, B), when compared to controls of the same age (measured in HAP) which were pollinated, but not infected or subject to a mock treatment (Fig. 11, A). By comparing the 48 HAP control (Fig. 11, A) with the picture of treated sample (Fig. 11, B), we can see that treated samples are in earlier stages of the development even though same time period has passed since pollination.

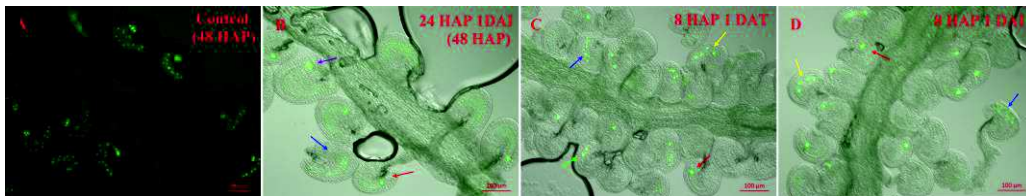


Figure 11. pAT2G40995:NLS-(3x)eGFP pollination-infection studies. Development delay of the ovules in treated samples when compared to control (B compared to A). A – all ovules are in stage of 48 HAP. Stages of the ovules (hours after pollination): red arrow – 0h/8h; green arrow – 10h; yellow arrow – 12h; blue arrow – 24h; violet – 48h. HAP – hours after pollination; DAI – days after infection; DAT – days after mock infection.

When comparing infection and mock treatments between each other (Fig. 11, C, D) we can see that both have ovules in very different developmental stages (from 0 HAP – 24 HAP) even though both pictures were taken 32 HAP (8 HAP combined with 1 DAT/I) and should have ovules mostly with eight nuclei (Fig. 11, C, D blue arrow; Fig. 7, F). This observation suggests that mock and infection treatments delay the development of the ovules.

In general, observations from pollination-infection studies further supported the need for a developmental characterization to investigate further the effect of pollination, infection and mock treatments.

Developmental studies

Developmental studies were perceived as necessary when initial pollination-infection studies were conducted and severe degradation and delay in development of the ovules were observed (see Fig. 10).

By looking at both 8 HAP and 24 HAP samples (Fig. 12; see deg. columns), percentage of degraded (deg.) ovules is increasing over time, with highest value being at 3rd day samples (Fig. 12, C, F; see deg. columns). This corresponds well with results gathered from pollination-infection pictures (Fig. 10). Thus confirming the previously proposed assumption that degradation increases over time.

Data also shows that degradation increases even if all samples were pollinated before the treatments, in contrast to previous results (Figs 10, 11). Here we see degradation increase (Fig. 12 from A to B to C and from D to E to F; see deg. columns) across all the samples. It is also important to point out that increase of the degradation is clearly visible in mock and infection treatment samples and to a lesser extent also in the control samples (Fig. 12, C, F; see deg. columns). This confirms that both treatments aggravate the degradation of the ovules.

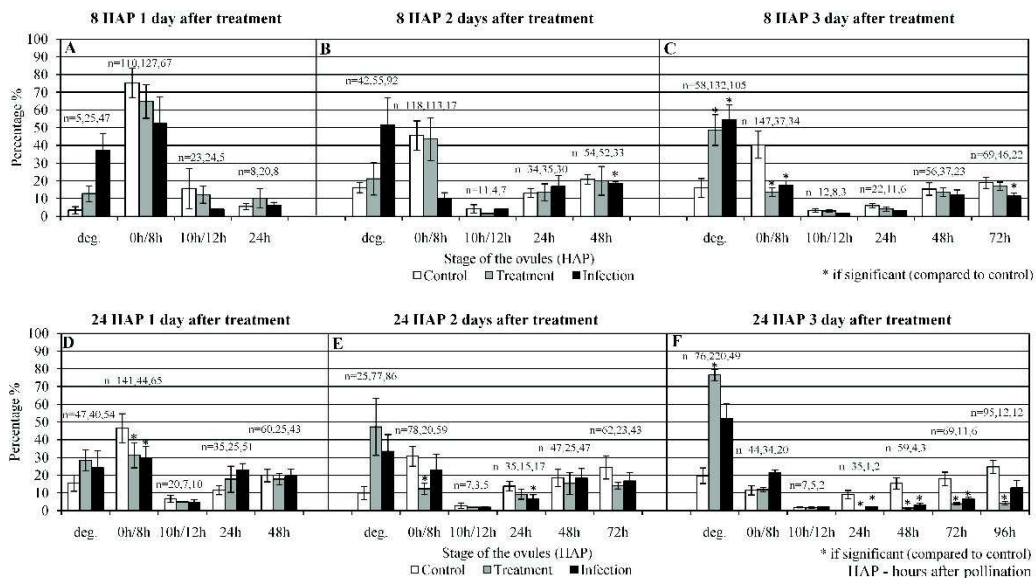


Figure 12. Results of developmental studies (A, B, C, D, E, F). HAP and control, mock or infection treatment effect on ovule development. Columns represent the percentage of stages ovules were in at given condition. Error bars represent the SD. Significance test – One-Way ANOVA; unequal variance t-Test: ($p < 0.05$). n – number of ovules at specific developmental stage counted within ca. 10 pistils (Example: figure A, from control (blue columns) samples in ca. 10 pistils 146 ovules were counted of which 5 were deg., 110 at 0h/8h, 23 at 10h/12h, 8 at 24h (for more detail see Fig. 7)).

Ovules at the stage 0h/8h (Fig. 12; see 0h/8h columns) show an opposite trend when compared to degrading ones (Fig. 12; see deg. columns), and decrease overtime (Fig. 12 from A to B to C and from D to E to F; see 0h/8h columns). The lowest percentage of 0h/8h stage ovules are in the 3rd day samples (Fig. 12, C, F; see 0h/8h columns). This makes sense since the 0h/8h ovules that generally look like and mostly are unpollinated ovules start to degrade over time. Interestingly in 8 HAP samples, infection treatment has highest degradation percentage (Fig. 12, C; see green deg. column), while for 24 HAP samples it was highest with mock treatment (Fig. 12, F; see red deg. column). It is not clear why time spent before treatment has such an effect, but it might be because at 8 HAP fertilization has not taken place in all ovules of a pistil (Gooh et al., 2015) making them perhaps more sensitive to infection.

When looking at samples, starting from 10h/12h to the oldest, we can see gradual increase of percentage by the stage in which the ovules were found (Fig. 12, B (see columns from 10h/12h to 48h), C (10h/12h to 72h), D (10h/12h to 48h), E (10h/12h to 72h), and F (10h/12h to 96h)). If we exclude degraded and 0h/8h data, we can see that the highest percentage ovules tend to be at the expected developmental stage corresponding to the treatment setting (Fig. 12, B, C, D, E, F; see from 10h/12h to oldest corresponding stage).

By performing statistical significance test (One-Way ANOVA; unequal variance t-Test) it becomes clear that mock and infection treatments delay the development of the ovules, at least in the 24 HAP 3 days after treatment samples (Fig. 12, F, see 24h, 48h, 72 h, 96 h columns). Overall, it is also clear that mock and infection treatments facilitate degradation of the ovules.

There is very little published information about ovule ageing, degradation and development delay in such specific conditions. Nonetheless, this study is giving a very interesting insight on how infection is affecting pollinated pistil and developing fruit. *Arabidopsis* is recognized as applicable model organism for translational research in cereals during *Fusarium* infection (Urban et al., 2002; Brewer & Hammond-Kosack, 2015). By improving the method so mock and infection treatments would not cause so much stress on samples and by looking for addition factors affecting the severity of degradation and development delay, as it has been done before (Carbonell-Bejerano et al., 2011), further research could prove to be very valuable in advancing the understanding of fungal infection effects on pollination, seed development and yield.

In this study three of GOI marker lines showed GFP signal in central cell and one in synergids. Many genes expressed in embryo sac are found to be essential for *Arabidopsis* reproduction and mutant analysis have identified multiple vital genes expressed in central cell, egg cell and synergids (Johnston et al., 2007). Central cells has vital role in pollen tube guidance (Chen et al., 2006; Li et al., 2015), while synergids trigger cell death after interacting with pollen tube (Sandaklie-Nikolova et al., 2007). Some CRPs have been recognized as essential in such reproduction events as pollen tube guidance (Li et al., 2015) in *Arabidopsis*. Even DEFLs are reported to have an important role in double fertilization (Okuda et al., 2009; Takeuchi & Higashiyama, 2012). Although our work lacks function studies, location of analyzed DEFLs is a good starting point for further investigation of these genes.

CONCLUSIONS

Marker lines of AT2G40995, AT5G38330 and AT1G60985 putative promoters are expressing GFP signal in the central cell of the embryo sac. Marker line of AT5G43285 putative promoter is expressing GFP signal in the synergids.

All four genes of interest (GOI) putative promoters – pAT2G40995, pAT5G38330, pAT5G43285 and pAT1G60985 – are downregulated after fertilization. Gene AT5G38330 promoter is upregulated 8 hours after pollination which is approximate time point of fertilization.

Mock and infection treatments are causing degradation and delay of development in treated ovules.

Method used for GFP signal quantification is reliable and can be used for investigating the conditions in which the GOIs are transcribed.

In future studies GFP signal quantification method can be used to advance our understanding of molecular basis of cereal resistance to FHB.

REFERENCES

- Beyer, M. & Aumann, J. 2008. Effects of *Fusarium* infection on the amino acid composition of winter wheat grain. *Food Chemistry* **111**, 750–754.
- Brewer, H.C. & Hammond-Kosack, K.E. 2015. Host to a stranger: *Arabidopsis* and *Fusarium* ear blight. *Trends Plant Sci.* DOI 10.1016/j.tplants.
- Carbonell-Bejerano, P., Urbez, C., Granell, A., Carbonell, J. & Perez-Amador, M.A. 2001. Ethylene is involved in pistil fate by modulating the onset of ovule senescence and the GA-mediated fruit set in *Arabidopsis*. *BMC Plant Biology*. DOI 10.1186/1471-2229-11-84.
- Chen, X., Steed, A., Harden, C. & Nicholson, P. 2006. Characterization of *Arabidopsisthaliana-Fusarium graminearum* interactions and identification of variation in resistance among ecotypes. *Mol Plant Pathol.* DOI 10.1111/j.1364-3703.2006.00349.x.
- De Wolf, E.D., Madden, L.V. & Lipps, P.E. 2003. Risk assessment models for wheat *Fusarium* head blight epidemics based on within-season weather data. *Phytopathology* **93**, 428–435.
- Ganz, T. 2003. Defensins: antimicrobial peptides of innate immunity. *Nature Reviews Immunology* **3**, 710–720.
- Gautam, P. & Dill-Macky, R. 2011. Type I host resistance and trichothecene accumulation in *Fusarium*-infected wheat heads. *American Journal of Agricultural and Animal Sciences* **6**(2), 231–241.
- Gooh, K., Ueda, M., Aruga, K., Park, J., Arata, H., Higashiyama, T. & Kurihara, D. 2015. Live-cell imaging and optical manipulation of *Arabidopsis* early embryogenesis. *Dev Cell* 2015. DOI 10.1016/j.devcel.2015.06.008.
- Hägglom, P. & Nordkvist, E. 2015. Deoxynivalenol, zearalenone, and *Fusarium graminearum* contamination of cereal straw; field distribution; and sampling of big bales. *Mycotoxin Research* **31**(2), 101–107.
- Huang, Q., Dresselhaus, T., Gu, H. & Qu, L. 2015. Active role of small peptides in *Arabidopsis* reproduction: expression evidence. *Journal of Integrative Plant Biology*. DOI 10.1111/jipb.12356.
- Johnston, A.J., Meier, P., Gheyselinck, J., Wuest, S.E., Federer, M., Schlagenhauf, E., Becker, J.D. & Grossniklaus, U. 2007. Genetic subtraction profiling identifies genes essential for *Arabidopsis* reproduction and reveals interaction between the female gametophyte and the maternal sporophyte. *Genome Biol.* **8**(10), R204.

- Li, H.J., Zhu, S.S., Zhang, M.X., Wang, T., Liang, L., Xue, Y., Shi, D.Q., Liu, J. & Yang, W.C. 2015. *Arabidopsis* CBP1 is a novel regulator of transcription initiation in central cell-mediated pollen tube guidance. *The Plant Cell* **27**, 2880–2893.
- McMullen, M., Jones, R. & Gallenberg, D. 1997. Scab of wheat and barley: a re-emerging disease of devastating impact. *Plant Dis.* **81**, 1340–1348.
- Okuda, S., Tsutsui, H. & Shiina, K. 2009. Defensin-like polypeptide LUREs are pollen tube attractants secreted from synergid cells. *Nature* **458**, 357–361.
- Rasband, W., Image, J. & Bethesda, M.D., 2009. USA: U.S. National Institutes of Health; 2009. Available: <http://rsb.info.nih.gov/ij/>.
- Sandaklie-Nikolova, L., Palanivelu, R., King, E.J., Copenhaver, G.P., Drews, G.N. 2007. Synergid cell death in *Arabidopsis* is triggered following direct interaction with the pollen tube. *Plant Physiol.* **144**(4), 1753–1762.
- Spalviņš, K. 2016. Expression and role of defensin-like peptides from *Arabidopsis* during fertilization and in the immune response to *Fusarium*. Master thesis. Riga, University of Latvia; pp. 80.
- Stotz, H., Spence, B. & Wang, Y. 2009. A defensin from tomato with dual function in defense and development. *Plant MolBiol.* **71**, 131–43.
- Takeuchi, H. & Higashiyama, T. 2012. A species-specific cluster of defensin-like genes encodes diffusible pollen tube attractants in *Arabidopsis*. *PLoS Biol.* DOI 10.1371/journal.pbio.1001449.
- Urban, M., Daniels, S., Mott, E. & Hammond-Kosack, K. 2002. *Arabidopsis* is susceptible to the cereal ear blight fungal pathogens *Fusarium graminearum* and *Fusarium culmorum*. *Plant J.* **32**(6), 961–73.
- Zimmermann, P., Hirsch-Hoffmann, M., Hennig, L. & Gruissem, W. 2004. GENEVESTIGATOR. *Arabidopsis* microarray database and analysis toolbox. *Plant Physiol.* **136**, 2621–2632.